Electromagnetic and thermal history during microwave heating

T. Santos, M.A. Valente, J. Monteiro, J. Sousa, L.C. Costa

▶ **To cite this version:**

HAL Id: hal-00789886
https://hal.archives-ouvertes.fr/hal-00789886

Submitted on 19 Feb 2013

Accepted Manuscript

Title: Electromagnetic and thermal history during microwave heating

Authors: T. Santos, M.A. Valente, J. Monteiro, J. Sousa, L.C. Costa
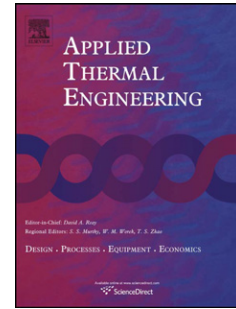
Electromagnetic and thermal history during microwave heating

T. Santos[1], M. A. Valente[1], J. Monteiro[1], J. Sousa[2], L. C. Costa[1#]

[1] Department of Physics and I3N, University of Aveiro, 3810-193 Aveiro, Portugal

[2] TEKA Portugal S.A., Estrada da Mota, 3834-909 Ílhavo, Portugal

Abstract

In microwave heating, the energy is directly introduced into the material resulting in a rapid and volumetric heating process with reduced thermal gradients, when the electromagnetic field is homogeneous. From those reasons, the microwave technology has been widely used in the industry to process dielectric materials. The capacity to heat with microwave radiation is related with the dielectric properties of the materials and the electromagnetic field distribution. The knowledge of the permittivity dependence with the temperature is essential to understand the thermal distribution and to minimize the non-homogeneity of the electromagnetic field. To analyse the history of the heating process, the evolution of the electromagnetic field, the temperature and the skin depth, were simulated dynamically in a ceramic sample. The evaluation of the thermal runaway has also been made. This is the most critical phenomenon observed in the sintering of ceramic materials because it causes deformations, or even melting on certain points in the material, originating the destruction of it. In our study we show that during the heating process the hot spot's have some dynamic, and at high temperatures most of the microwave energy is absorbed at the surface of the material. We also show the existence of a time-delay of the thermal response with the electromagnetic changes.

[#] Corresponding author: Luís Cadillon Costa, e_mail: kady@ua.pt; phone: +351234370944; fax:+351234378197.

1. Introduction

In contrast with the conventional technology to sinter materials, where they are heated by conduction, convection and radiation, the material processed in a microwave oven is heated through the interactions of the material with the microwave radiation. The heat is produced by interaction of the microwave with the material, so the heating process is more volumetric and consequently, it is a faster process because higher heating rates are possible without excessive temperature gradients. When the main factors are controlled, it is possible to have a final product in shorter time, with higher cleaning environment, greater productivity in less space, and decrease of heat losses, and, consequently, reducing the manufacturing costs [1]. Along economical advantages, with microwave technology it is possible to have a product with greater uniformity, enhanced densification rate, finer and more uniform grain structure and better mechanical properties [2, 3]. An intrinsic aspect, in the microwave processing, is the heating rate changing the characteristics of different materials during the heating process [3, 4].

Due to these advantages we observe, nowadays, a significant increase in the research on microwave processing of materials in several areas, particularly, ceramics [5], polymers [6], chemistry [7], hazardous waste [8], etc. In the literature are presented also researches in selective heating [9] and casting metals [10].

The electric field distribution is the major factor that influences how materials undergo processing in a microwave oven. To calculate the different distributions is then crucial to understand the complex phenomenon of the dielectric heating of materials under a microwave radiation in order to avoid overheating points that can destroy the material at a local level. This phenomenon, referred in the literature as thermal runaway, has been reported in a variety of materials, like zirconia [11], alumina [12] and nylon [13]. To understand and control this behaviour, a perspective of the electromagnetic-thermal

history during the heating process is essential. To accomplish our objective we have to model mathematically the microwave electromagnetic field, using the Maxwell equations and the boundary conditions, which can be solved using the Finite Element Method [14, 15].

Several numerical studies have been made in order to describe the most critical aspects that influence and govern the processing of materials with microwave radiation. In [16] the authors simulated one cylindrical sample exposed to a uniform and constant microwave field in a standard RG 112-U waveguide (single-mode cavity). In that study they demonstrated that the thermal runaway is a function of the thermal conductivity, the convective heat transfer, the surrounding temperature, the intensity of the electromagnetic field, the permittivity, and the radius of the sample. Others numeric's studies demonstrated some aspects that may influence the heating process, as, the position of the waveguide relatively to the cavity [17], the variation in the frequency of the microwave radiation, the complex permittivity, $\varepsilon_r^* = \varepsilon_r^{'} - i\varepsilon_r^{''}$ [18], the position of the microwave radiating antenna relatively to the waveguide, the effects of the cavity dimensions [19] and the influence of mode stirrers [19, 20]. The optimization, versatility and velocity in the results estimation of the numerical analysis have evident advantages compared with experimental measurements, but an experimental validation is required [21, 22]. A more complex model has been developed describing the evolution of the density and the grain size during the heating process [23].

The study of the microwave systems is approached in the hypothesis of the absence of losses on the boundary, admitting that the walls are a perfect conductor. Nevertheless, if there are some losses in the conductive walls, these will be small enough, in order to not affect significantly the distribution of the electromagnetic field [24].

This paper presents a 2D simulation of the electromagnetic field distribution inside a microwave oven, and the corresponding thermal distribution in order to understand the influence of the dielectric properties variations along the heating process.

2. Experimental

A 2D microwave model has been developed using the COMSOL Multiphysics v4.1 software to simulate the electromagnetic field and the thermal distribution, inside a square oven with 26 cm sides and with a circular ceramic sample, 4.5 cm radius, in the centre of the cavity. In figure 1 we present the schematic of the cavity, the WR-340 waveguide, the ceramic material and the representation of 4 points (pt1, pt2, pt3, pt4) and a diameter where the heating process was studied.

The excitation port of the waveguide is powered by 1 kW at a frequency of 2.45 GHz, in the fundamental mode $TE_{1,0}$.

The cavity and waveguide are filled with air whose $\mu_r = \varepsilon_r = 1$, and the sample has density $\rho = 8.8$, specific heat coefficient $C_p = 1100$ ($Jkg^{-1}K^{-1}$), thermal conductivity k=0.2 ($WK^{-1}m^{-1}$), dc electrical conductivity $\sigma_{dc} = 10^{-7}$ (Sm^{-1}). Only the relative complex permittivity has been considered dependent with temperature, where $\varepsilon_r^*(\omega,T) = \varepsilon_r^{'}(\omega,T) - i\varepsilon_r^{''}(\omega,T)$. In figure 2 we present the complex permittivity dependence with the temperature of the sample.

The electric field E, in the oven is given by the following equation

$$\nabla \times \mu_r^{'^{-1}}(\nabla \times E) - k_0^2\left(\varepsilon_r^{'} - \frac{i\sigma_{ac}}{\omega\varepsilon_0}\right)E = 0 \qquad (1)$$

where σ_{ac} is the ac electrical conductivity and k_0 is the wave-vector in free space.

The microwave power density (Wm^{-3}) absorbed by the material can be expressed by equation

$$P = \frac{1}{2}\left[\left(\sigma_{dc} + \omega\varepsilon_r^{''}\right)E^2 + \omega\mu_r^{''}H^2\right] \qquad (2)$$

where E and H are the absorbed electric and magnetic fields. In our case, the nonmagnetic material used in this work eliminates the need of using the second term of this equation.

At the macroscopic level, the dielectric properties controls the microwave process of a wide range of non-magnetic materials through the quantitative relationships of the absorbed power per unit volume, P, and the skin depth, D_p, [25]

$$D_p = \sqrt{\frac{2}{\pi f \sigma_{ac}}} \qquad (3)$$

Coupling the absorbed electromagnetic energy with the thermal energy generated in the material, considering the time dependence, the heating rate in the material due to the absorption of the microwave radiation (Ks^{-1}) is expressed by

$$\rho C_p \frac{\partial T}{\partial t} = k \nabla^2 T + P \qquad (4)$$

3. Results and discussion

In figure 3 we represent the heating process where is possible to observe an increase in temperature in areas where the field is greater. This occurs because as the temperature increases those areas have higher ability to absorb microwave energy, which leads to variations of the permittivity along the sample. If the dielectric losses increases strongly (figure 2), those areas observe an abrupt increase of temperature, which may lead to thermal runaway phenomenon, as showed in figure 3. This unstable accelerated heating appears mainly due to the dependency of the complex permittivity and thermal conductivity with temperature.

In the case study, we observe a decreasing of the electromagnetic field amplitude in the centre of the sample (pt1), principally due to the low skin depth after sixty minutes,

(figure 4). Consequently is observed a lower energy absorption in this point, with a temperature decreasing. After one hundred and ten minutes the temperature grows again, mainly due the energy transfer to the centre of the sample by thermal conduction from others hot spots. Beyond the thermal runaway, before sixty minutes, is evident a gradient between the centre point (pt1) and the other three points. After one hundred and twenty minutes, we observe a gradient between pt3 and the rest. These gradients and the thermal runaway phenomenon may give rise to deformation and even deterioration of the material. It is clear that the temperature at the central point after one hundred and fourty minutes is lower than the temperature of the others. These aspects are explained by the variation of the power density absorbed in pt1, pt2, pt3 and pt4 along the heating process (figure 5) and due to the changing of the electromagnetic field pattern with the variation of the complex permittivity (figure 6).

We must have into account that ceramic materials with $\varepsilon_r^{''}$ between 10^{-2} and 5 are good absorbers of microwaves. For $\varepsilon_r^{''}<10^{-2}$ they have a low absorption capability and for $\varepsilon_r^{''}>5$ most of the energy is absorbed at the surface [26]. Due to that, as the temperature increases, D_p decreases. In the beginning we have a D_p value of the order of 1.4 m and during the heating process it decreases to the order of millimetre. After one hundred minutes D_p decreases to values close to zero, consequently most of the energy is absorbed in the first millimetres of the sample.

In figure 6 we show some stages of the electromagnetic and thermal history.

We can observe that the electric field distribution is far from being uniform, and it is obvious that along the heating process the variation of the electromagnetic field distribution, which gives rise to a subsequent change in the hot spots, is not instantly. As the material heat's up, the dielectric characteristics changes (in our case both, $\varepsilon_r^{'}$ and $\varepsilon_r^{''}$ increase with temperature), with lower electric field penetrating into the sample.

In figure 7 we observe the delay present in the thermal profile. During the heating process when the electromagnetic field pattern changes, the thermal variations do not occur at the same rate. Looking to the electromagnetic pattern at t = 90 minutes it is clearly the existence of a maximum of |E| at the bottom of the sample with an amplitude equal to the maximum observed in the centre, and in the top of the sample. However, only after some time we began to observe an increase of temperature in the bottom of the sample. In a certain moment the electromagnetic power in different areas of the sample is the same (or very close), but the temperature in those areas is very different, so we do not expect a sudden temperature equality between them. In the top of the sample (pt4) this is not observed because the difference between this point and the centre is about 300 °C.

A complementary look of this analysis is demonstrated in figure 8, where it is possible to observe the "delay" between the electromagnetic field and temperature in the sample, over the path drawn in figure 1.

Supposing that we do not know the thermal history of the sample, if we look to the norm of the electric field amplitude for t = 90 minutes (figure 8b) we should expect that the hottest point is at ø = 0.08 m (ø is the diameter of the sample). However considering the past of the sample we observe that between this point and the real hottest point (at ø = 0.04 m) exist a difference of approximately 400 °C. Only after some time this two points have close temperatures. This happens for t = 120 minutes, as observed in figure 8d. The same discrepancy is verified for ø = 0.00 m. It should be noted that between fifty eight minutes and ninety minutes, |E|, for ø = 0.00 m, is slighter lower than for ø = 0.08 m, but the temperature is higher. This is explained by the fact that the absorbed power is a function of the electromagnetic field, the frequency (that is constant) and $\varepsilon_r^{''}$.

During the heating process, this last term, changes along the sample and it has a higher value in those regions where the temperature is higher. Hence, to fully understand the microwave heating process, we need to know the electromagnetic and thermal history, and also the complex permittivity variation with temperature along the sample.

For all the domains we have adopted a triangular mesh. To create the mesh we must fulfil the Nyquist criterion of at least two elements per wavelength. So, for each domain we adopted a maximum element size given by $\lambda_D = c \big/ 6 f \sqrt{\varepsilon'_{rD} \mu'_{rD}}$, where c, f, ε'_{rD} and μ'_{rD} are the free space speed of light, the frequency, the dielectric constant and the relative permeability in the respective domain, respectively. In the air we have $\lambda_D = 0.02$ m, and in the ceramic material, $\lambda_D = 0.0056$ m.

The mesh quality is related to the aspect ratio, which means that anisotropic elements can get a low quality measure even though the element shape is reasonable. For triangular elements, COMSOL Multiphysics computes the mesh quality q ($0 < q < 1$) as [27]

$$q = \frac{4\sqrt{3}A}{h_1^2 + h_2^2 + h_3^2} \tag{5}$$

where A is the area and, h_1, h_2 and h_3 are the side lengths of the triangle. If $q > 0.3$ the mesh quality should not affect the solution's quality.

In our case we have 1559 triangular elements, a minimum element quality of 0.8455 and an average element quality of 0.9776, confirming the mesh quality.

4. Conclusions

To illustrate the usefulness of the numerical technique, the thermal runaway in a ceramic material was simulated. This phenomenon presents a challenge for microwave engineers, since sample cracking are often exhibited due to huge thermal gradients.

The results, simulated with the COMSOL Multiphysics v4.1, showed that due to the temperature dependence of the real and imaginary parts of the permittivity, the electromagnetic field pattern changes during the heating, and so, the hot spot's have some type of dynamics. For high temperatures (T > 1000 ºC which implies t > 100 min) the skin depth have an appreciably decreases, and consequently the microwave energy is mainly absorbed at the surface of the sample. When the electromagnetic field changes the thermal changes do not occur at the same rate, existing a significant delay.

To manage with efficiency all the heating process we must control not only the electromagnetic field heterogeneity, but also the thermal history.

Acknowledgements

References

[1] W.S. Sutton, Microwave processing of ceramics-an overview, in: R.L. Beatty, W.S. Sutton, M.F. Iskander (Eds.), Microwave Processing of Materials III, Vol. 269, Materials Research Society, Pittsburgh, 1992, 3-20.

[2] J.D. Katz, R.D. Blake, Microwave sintering of multiple alumina and composite components, Americ. Ceram. Soc. Bull. 67 (1988) 1656-1661.

[3] Z. Xie, J. Yang, X. Huang, Y. Huang, Microwave processing and properties of ceramics with different dielectric loss, J. Europ. Ceram. Soc. 19 (1999) 381-387.

[4] C. Zhao, J. Vleugels, C. Groffils, P.J. Luyaert, O. van Der Biest, Hybrid sintering with a tubular susceptor in a cylindrical single-mode microwave furnace, Acta Mater. 48 (14) (2000) 3795-3801.

[5] C. Leonelli, G.C. Pellacani, C. Siligardi, P. Veronesi, Microwave assisted burn-out of organic compounds in ceramic systems, in: H. Mandal, L. Öveçoglu (Eds.), Key Engineering Materials, Vols. 264-268, Trans Tech Publications, Switzerland, 2004, 739-742.

[6] V.K. Varadan, V.V. Varadan, Microwave joining and repair of composite materials, Polym. Eng. Sci. 31 (7) (1991) 470-486.

[7] C.O. Kappe, Controlled microwave heating in modern organic synthesis, in: Wiley-VCH Verlag GmbH & Co. KGaA (Eds.), Angewandte Chemie International Edition, Vol. 43, A Journal of the Gesellschaft Deutscher Chemiker, Weinheim, 2004, 6250-6284.

[8] S.J. Oda, Microwave applications to process nuclear and hazardous waste, in: D.E. Clark, W.R. Tinga, J.R. Laia (Eds.), Microwaves: Theory and Applications in Materials Processing II, Ceramic Transactions, Vol. 36, The American Ceramic Society, Westerville, 1993, 73-79.

[9] M. Tanaka, H. Kono, K. Maruyama, Selective heating mechanism of magnetic metal oxides by a microwave magnetic field, Phys. Rev. B 79 (2009) 104420.

[10] M.H. Awida, N. Shada, B. Warren, E. Ripley, A.E. Fathy, Modelling of an industrial microwave furnace for metal casting applications, in: Institute of Electrical and Electronics Engineers (Eds.), Proceedings Microwave Symposium Digest, Institute of Electrical and Electronics Engineers, MTT-s International, 2008, 221-224.

[11] M. Arai, J.G. Binner, G.E. Carr, T.E. Cross, High temperature dielectric measurements on ceramics, in: R. L. Beatty, W. S. Sutton, M. F. Iskander (Eds.),

Microwave Processing of Materials III, Vol. 269, Materials Research Society, Pittsburgh, 1992, 611-618.

[12] D.L. Johnson, D.J. Skamser, M.S. Spotz, Temperature gradients in microwave processing: Boon and bane, in: D. E. Clark, W. R. Tinga, J. R. Laia (Eds.), Microwaves: Theory and Applications in Materials Processing II, Ceramic Transactions, Vol. 36, The American Ceramic Society, Westerville, 1993, 133-146.

[13] K.G. Ayappa, H.T. Davis, E.A. Davis, J. Gordon, Two-dimensional finite element analysis of microwave heating, Amer. Inst. Chem. Eng. J. 38 (1992) 1577-1592,.

[14] W. Fu, A. Metaxas, Numerical prediction of three-dimensional power density distribution in a multimode cavity, J. Microwave Pow. Electr. Ener. 29 (2) (1994) 67-75.

[15] L. Zhou, V.M. Puri, R.C. Anantheswaran, G. Yeh, Finite element modelling of heat and mass transfer in food materials during microwave heating - Model development and validation, J. Food Eng. 25 (1995) 509-529.

[16] G. Roussy, J. Mercier, Temperature runaway of microwave irradiated materials, J. Appl. Phys. 62(4) (1987) 1167-1170.

[17] L. Bandici, T. Leuca, P.A. Palade, Some aspects regarding the optimization of the electromagnetic field propagation in microwave structures, J. Electr. Electr. Eng. (2009) 7-12.

[18] T. Santos, L.C. Costa, M.A. Valente, J. Monteiro, J. Sousa, 3D electromagnetic field simulation in microwave ovens: a tool to control thermal runaway, IEEE Spectrum (2011), In Press.

[19] K. Umetsu, Y. Tomizawa, Designing of microwave applicators by electromagnetic wave analysis, Shinn. Giho 379 (2003) 65-69.

[20] J.M. Cabrera, A.D. Morcillo, A.L. Guerrero, Electromagnetic modelling activities at the technical university of Cartagena: a review, Proceedings of 10th seminar computer modelling & microwave power engineering, Modena, Italy, 2008, 7-11.

[21] H. Ju, Q. Zhao, Simulation and experimental method for microwave oven, J. Electr. Sci. Tech. China 7 (2) (2009) 188-191.

[22] J.D. Newman, L. Walsh, R. Evans, T. Tjolen, O.M. Andrade, M.F. Iskander, K.J. Bunch, Experimental validation of numerical simulations of the microwave sintering process, in: D. E. Clark, W. R. Tinga, J. R. Laia (Eds.), Microwaves: Theory and Applications in Materials Processing II, Ceramic Transactions, Vol. 36, The American Ceramic Society, Westerville, 1993, 229-237.

[23] H. Riedel, J. Svocoba, Simulation of microwave sintering with advanced sintering models, in: M. Willert-Porada (Eds.), Advances in microwave and radio frequency processing, Part III, Springer, New York, 2006, 210-216.

[24] T. Leuca, L. Bandici, P.A. Palade, I. Stoichescu, Numerical Analysis of the Electromagnetic Field in Microwave Processing of Forest Fruits, J. Electr. Electr. Eng. 1 (2009) 64-67.

[25] P.R. Karmel, G.D. Colef, R.L. Camisa, Introduction to Electromagnetic and Microwave Engineering, John Wiley and Sons, Oxford, 1998.

[26] D.E. Clark, D.C. Folz, What is Microwave processing, http://personnel.univ-reunion.fr/lanson/typosite/fileadmin/documents/pdf/TMO_M2/ Projet/Microwave_Solutions_for_Engineers_Introduction.pdf. Last acceded: 11/1/2011.

[27] COMSOL Multiphysics User's Guide version 3.5a, 2008, 370-372.

Figure captions

Figure 1 – Microwave 2D cavity oven and the sample to process.

Figure 2 – Dielectric characteristics.

Figure 3 – Temperature distribution with time.

Figure 4 – Skin depth in the sample.
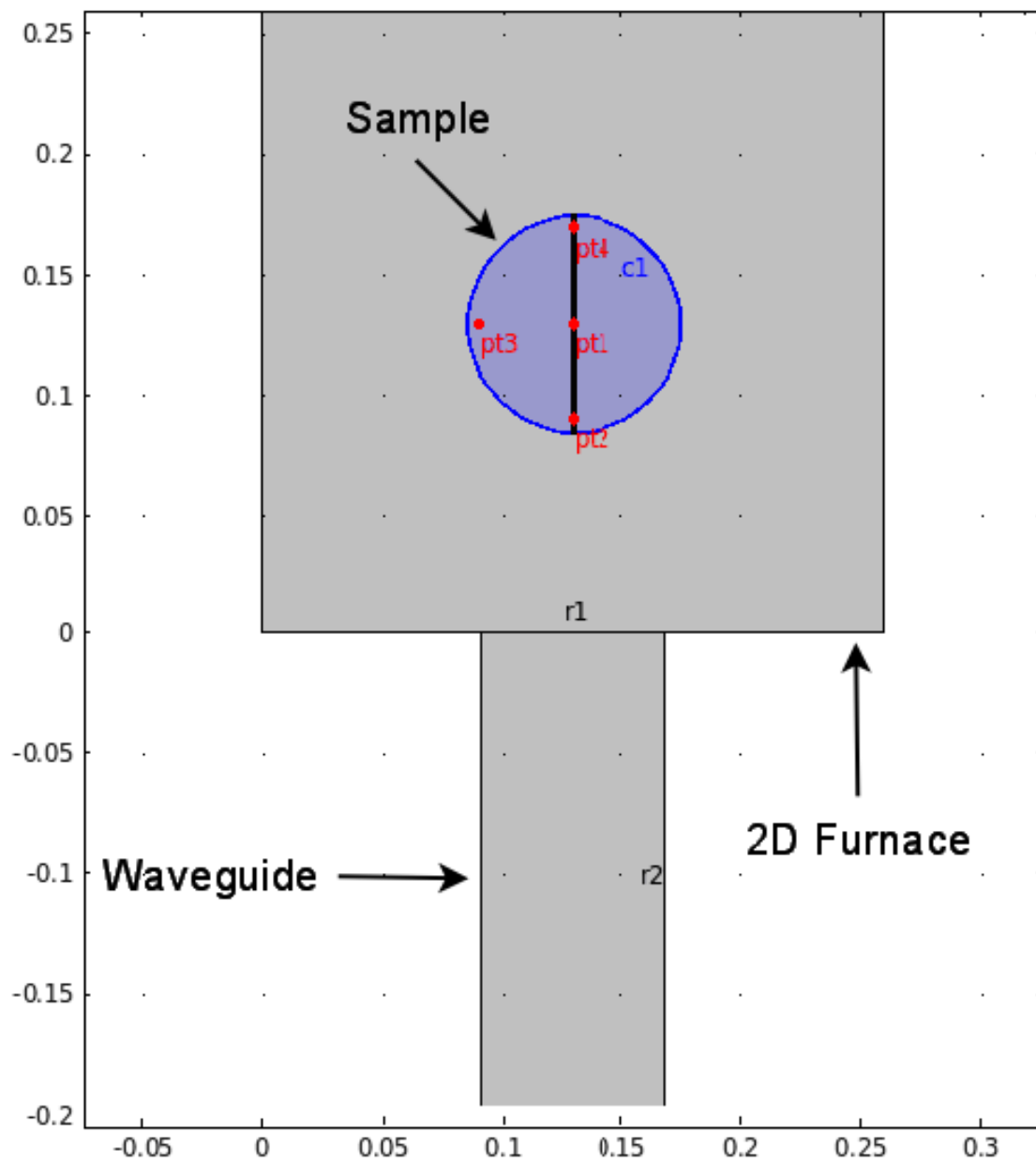
Figure 5 – Power absorbed by the material.

Figure 6 – Electromagnetic and thermal progress along the heating progress, for $t \leq 80$ min [a) |E| (V/m) for 4.17 min, b) T (ºC) for 4.17min, c) |E| (V/m) for 25 min, d) T (ºC) for 25 min, e) |E| (V/m) for 58 min, f) T (ºC) for 58 min, g) |E| (V/m) for 80 min, h) T (ºC) for 80 min].

Figure 7 – Electromagnetic and thermal history, for $t \geq 90$ min [a) |E| (V/m) for 90 min, b) T (ºC) for 90min, c) |E| (V/m) for 100 min, d) T (ºC) for 100 min, e) |E| (V/m) for 120 min, f) T (ºC) for 120 min].

Figure 8 – Electromagnetic and thermal history over the line, along the diameter of the sample, traced in figure 1 [a) for 58 min, b) for 90 min, c) for 100 min, d) for 120 min].

- Electromagnetic field, the temperature and the skin depth were simulated dynamically.
- The evaluation of the thermal runaway has been made.
- A time-delay of the thermal response with the electromagnetic changes exists.

Surface: Electric field norm (V/m) at min = 4.17

Surface: Temperature (degC) at min = 4.17

Surface: Electric field norm (V/m)   at min = 25

c)

Surface: Temperature (degC) at min = 25

Surface: Electric field norm (V/m) at min = 58

e)

Surface: Temperature (degC) at min = 58

f)

Surface: Electric field norm (V/m) at min = 80

g)

Surface: Temperature (degC) at min = 80

Surface: Electric field norm (V/m) at min = 90

a)

Surface: Temperature (degC) at min = 90

b)

Surface: Electric field norm (V/m) at min = 100

c)

Surface: Temperature (degC) at min = 100

d)

Surface: Electric field norm (V/m) at min = 120

e)

Surface: Temperature (degC) at min = 120

c)